**Conference**
**on Modelling Fluid Flow (CMFF'25)**
**Radisson Blu Béke Hotel** August 26-29, 2025 Budapest / Hungary

Conference on Modelling Fluid Flow CMFF'25
The 19th event of the International Conference Series
on Fluid Flow Technologies held in Budapest since 1959

# Conference Proceedings

**Edited by J. Vad**

**Department of Fluid Mechanics** / Faculty of Mechanical Engineering
**Budapest University of Technology and Economics**
**2025**

**Proceedings of the Conference on Modelling Fluid Flow**
**CMFF'25**

**Edited by J. Vad**

Department of Fluid Mechanics,
Budapest University of Technology and Economics
2025 Budapest, Hungary

**ISBN 978-615-112-002-6**

Published by the Department of Fluid Mechanics,
Faculty of Mechanical Engineering,
Budapest University of Technology and Economics

Address:
Bertalan Lajos 4-6., H-1111 Budapest, Hungary
www.ara.bme.hu

INFLUENCE OF A SCANNING BOX ON THE SETTLING TIME OF MULTI-HOLE PRESSURE PROBES 9
HAZARD PREDICTION MODELS FOR BATTERY MODULE AND PACKS: FLAMMABILITY, PARTICLE IGNITED VENT GAS , ARCING WITHOUT AND WITH PARTICLES 18
MULTI-OBJECTIVE DESIGN OPTIMIZATION OF A VARIABLE-PITCH AXIAL FLOW FAN BY USING CFD-BASED META-MODEL 29
MODELLING OF PARAMETRIC OSCILLATIONS IN FLOATING BODIES 34
LAMINAR – TURBULENT TRANSITION IN HELICALLY COILED REACTORS. AN EXPERIMENTAL STUDY WITH HIGH-SPEED PIV 41
REDESIGNED ADJUSTABLE DIAPHRAGM FOR CONTROLLIN-G AND MITIGATING THE SWIRLING FLOW INSTABILITIES FROM THE CONICAL DIFFUSER OF HYDRAULIC TURBINES 49
MOBILE SEPARATION OF COMPLEX OIL-WATER MIXTURES WITH AN ADAPTED PITOT PUMP 56
PREDICTIONS OF PARTICLE TRAJECTORY RESPONSE TO REYNOLDS NUMBER IN TURBULENT CHANNEL FLOWS USING ARTIFICIAL NEURAL NETWORKS 64
ENHANCING PREDICTIVE ACCURACY OF TURBULENT SUBCOOLED FLOW BOILING USING LES 72
LASER-OPTICAL VALIDATION AND COMPARATIVE ANALYSIS OF NUMERICAL HEAT TRANSFER MODELS FOR SINGLE NOZZLE IMPINGEMENT FLOWS 80
A CFD STUDY ON THE EFFECT OF DEFORMABLE BLADES ON CENTRIFUGAL PUMP PERFORMANCE 90

ASSESSMENT OF RANS TURBULENCE MODELLING APPROACHES FOR POLLUTANT DISPERSION IN VEGETATED STREET CANYONS USING PERIODIC BOUNDARY CONDITIONS 98
THE EFFECT OF BUBBLE PARAMETERS ON THE MIXING IN A BUBBLE COLUMN WITH COUNTER-CURRENT LIQUID FLOW 109
MODULATING VORTEX DYNAMICS AROUND CIRCULAR CYLINDER VIA ASYMMETRIC CROSS-SECTIONAL PROFILE MORPHING: A COMPARATIVE STUDY OF CYLINDRICAL AND ELLIPTICAL CONFIGURATIONS 118
A CFD STUDY ON DEPOSITION EFFICIENCY IN CASE OF INHALED AEROSOL MEDICATION 126
INFLUENCE OF CUT-BACK LEADING EDGES ON EFFICIENCY AND FUNCTIONALITY FOR AN OPTIMIZED SEMI-OPEN 2-CHANNEL IMPELLER 134
DYNAMICS AND COLLISION OF NON-SPHERICAL ELLIPSOID PARTICLES IN TURBULENT CHANNEL FLOW 142
EXPLORING TRANSIENT INSTATIONARITIES OF MECHANICAL LOAD IN THE OPERATION OF WASTEWATER PUMPS 150
THE EFFECT OF HOUSING RECESS GEOMETRY ON FIBER ENTRY INTO THE BACK SHROUD CAVITY OF A WASTEWATER PUMP 158
DIRECT NUMERICAL SIMULATION OF THE JET ATOMIZATIO-N PROCESS OF SHEAR THINNING GEL FUEL 166
MOLECULAR DYNAMICS SIMULATION OF THE RHEOLOGIC-AL BEHAVIOUR OF GEL FUELS 173
EFFICIENT RADIAL-AXIAL JET FOR IMPROVING THE FLEXIBI-LITY IN OPERATION OF HYDRAULIC TURBINES 178

OPTIMISATION OF INLET GUIDE VANE FOR LARGE AXIAL FANS BASED ON BIG DATA ANALYSIS 186
ESTIMATION OF RELATION BETWEEN PRESSURE DIFFERENCE AND FLOW RATE IN A FRANCIS-TURBINE SPIRAL CASE USING NUMERICAL COMPUTATION 194
DEFINITION AND COMPUTATION OF A FLUTTER SAFETY MARGIN FOR QUADCOPTERS BY CHAINING TOGETHER MULTIPLE 2-DOF AEROELASTIC MODELS 200
DEVELOPMENT OF A CYLINDRICAL-BLADE WIND TURBINE DRIVEN BY A NECKLACE VORTEX 207
A THROMBOSIS MODEL FOR BLOOD-CONTACTING MEDICAL DEVICES 213
STUDY OF THE MIXING PERFORMANCE OF CURVED BLADE TURBINES IN A SOLID-LIQUID DUAL IMPELLER STIRRED SYSTEM 221
MINIMIZING SEDIMENTATION IN ROUND WASTEWATER PUMPING STATIONS WITH THE ASSISTANCE OF PHYSICAL MODELS 229
CFD MODELLING OF THE THERMO- AND HYDRODYNAMIC C-APABILITIES OF LONG-NECKED PLESIOSAURS (REPTILIA, S-AUROPTERYGIA) 236
A 0D-3D MODEL FOR THE ANALYSIS OF THE TRANSIENT THERMAL BEHAVIORS OF AN ELECTRIC POWER TRAIN 244
EQUILIBRIUM POSITIONS AND DYNAMIC BEHAVIOR OF THERMAL PROLATE PARTICLES IN SHEAR FLOW: INFLUENCE OF PARTICLE SIZE 252
A NOVEL SPH MODEL FOR THROMBUS FORMATION 258
GAS ACCUMULATION BEHAVIOR IN DIVERGING CHANNELS WITH GROOVES AND BARS OF VARYING SIZES 266

NUMERICAL ANALYSIS OF THE DECELERATED SWIRLING FLOW REGIMES OBTAINED BY USING A MAGNETORHEOLOGICAL CONTROL DEVICE 274
MODELING OF FACE MASK FLOW AND DROPLET FILTRATION 281
THE CFD-BASED DESIGN OF A BYPASS TUNNEL TO PROVIDE THE CROSS-FLOW USED IN THE CASE OF BLADE CASCADE AEROELASTIC STUDY 289
PIPE FLOW ANALOGY IN A PLANAR MASS-SPRING-DAMPER SYSTEM 295
INVESTIGATION OF RADIUS RATIO EFFECTS ON VELOCITY STATISTICS IN ANNULAR PIPE FLOW USING ONE-DIMENSIONAL TURBULENCE 302
COMBUSTION- AND POLLUTANT-MODELLING OF DIMETHYL ETHER IN A SWIRL-STABILIZED COLD AIR BURNER 310
DEVELOPMENT OF A CEREBRAL PERIPHERAL VASCULATURE MODEL FOR QUANTITATIVE ASSESSMENT OF COLLATERAL BLOOD FLOW USING SPECT AND 4D FLOW MRI 318
EFFECTS OF WALL SLIP ON LARGE-SCALE FLOW IN TURBULENT RAYLEIGH–BÉNARD CONVECTION 326
NUMERICAL INVESTIGATION ON THE INFLUENCE OF INTERNAL CAROTID ARTERY GEOMETRY ON WALL SHEAR STRESS DISTRIBUTION 334
A CONSISTENT APPROACH TO ATMOSPHERIC BOUNDARY LAYER SIMULATIONS USING THE K-ω SST MODEL 341
LES AND DES OF FLOW AND ICE ACCRETION ON WIND TURBINE BLADES 350

ODTLES: LARGE-EDDY SIMULATION WITH AUTONOMOUS STOCHASTIC SUBGRID-SCALE MODELING APPLIED TO TURBULENT DUCT FLOW 358
NUMERICAL ANALYSIS OF SWIRLING FLOW INDUCED BY AXIAL FAN 366
FLOW DIVERTER TREATMENT FOR INTRACRANIAL MEDIA B-IFURCATION ANEURYSMS: CHALLENGING THE PREDICTIVE ROLE OF MORPHOLOGY AND HEMODYNAMICS 374
NUMERICAL INVESTIGATION OF A LIFTED METHANE/AIR JET FLAME USING STOCHASTIC MAP-BASED TURBULENCE MODELING 382
NUMERICAL INVESTIGATION OF LIQUID EMBOLIZATION FOR INTRAVASCULAR TREATMENT USING A PARTICLE METHOD 390
DEVELOPMENT OF THE TURBULENT SWIRLING FLOW VELOCITY PROFILES IN THE AXIAL FAN JET 397
EVALUATING THE PROBABILITY OF INFECTION IN A UK HOSPICE THROUGH A CFD DRIVEN METRIC 403
NUMERICAL MODEL DEVELOPMENT AND ANALYSIS OF A DROP-ON-DEMAND INKJET APPLICATION 412
A NOVEL EULERIAN-LAGRANGIAN MULTI-SCALE METHOD FOR CAVITATING FLOW IN AN INJECTOR NOZZLE 421
LOW-AMPLITUDE ACOUSTIC MODULATION AS A TOOL FOR CONTROLLING THE VORTEX STRUCTURES OF THE TURBULENT AXISYMMETRIC AIR JET 428
BEM SIMULATION OF AN EXPANDING / CONTRACTING BUBBLE IN VISCOELASTIC FLUIDS 439
A COMPREHENSIVE ANALYSIS OF VARIABLE INLET GUIDE VANE ON CAVITATION AND HYDRAULIC PERFORMANCE OF AN AXIAL-FLOW PUMP 446

SPHERICAL STABILITY AND BREAKUP LIMIT OF OSCILLATIN-G MICROBUBBLES 455
FLUID MECHANICS OF CEREBRAL THROMBI 463
MODELLING THE TRANSPORT OF OXYGEN IN THE HUMAN VASCULAR SYSTEM 471
MODELLING THE METABOLIC AND MYOGENIC CONTROL IN HUMAN BLOOD CIRCULATION 477
MULTIPHASE MODEL OF THE MELT BLOWING PROCESS IN MULTI-HOLE NOZZLES 484
CAVITATION BUBBLE NEAR A WALL: SENSITIVITY TO MODELING CONDITIONS 492
SUPERPOSITION OF SECONDARY FLOWS INSIDE ARTIFICIAL GEOMETRIES 501
GEOMETRICAL OPTIMIZATION OF RECTANGULAR MVGS DELAYING BOUNDARY LAYER TRANSITION OVER A FLAT PLATE 508
DESIGN AND DEVELOPMENT OF AN AUTOMATIC PUMP TEST RIG FOR CONDITION MONITORING OF MECHANICAL SEALS 516
SIMULATION AND CHALLENGES FOR A LOW SPECIFIC SPEED PELTON TURBINE 525
APPLICATION RANGES OF THE HAGEN-POISEUILLE LAW TO MODEL NON-NEWTONIAN FLUID-FILLED DAMPERS 535
EVALUATION OF CAROTID PLAQUE MORPHOMETRY AND H-EMODYNAMICS 543
IMPACT OF WAVE DIRECTIONALITY AND INTER-DEVICE SPACING ON THE PERFORMANCE OF WAVE ENERGY CONVERTER ARRAYS 550

EXPERIMENTAL AND NUMERICAL INVESTIGATIONS OF NOZZLE SPACING EFFECTS ON FLOW CHARACTERISTICS OF TRIPLE RECTANGULAR FREE JETS 557
AN APPLICATION OF MACHINE LEARNING TO COMPUTE THERMOCHEMISTRY OF REACTIVE FLOWS: A MIXTURE OF EXPERTS APPROACH 565
COMBINING THE PARTIALLY STIRRED REACTOR WITH A DEM DESCRIPTION: THE PYROLYSIS OF BIOMASS 573
USING JACOBI METHOD TO SOLVE THE TWO-EQUATION TURBULENCE MODEL FOR PARALLELIZATION ON GPU COMPUTING SYSTEM 581
EXPERIMENTAL AND NUMERICAL INVESTIGATION OF THE TURBULENT SWIRLING FLOW IN PIPE BEHIND THE AXIAL FAN IMPELLER 588
A NEW VISCOSITY FORMULATION FOR IMPROVED TURBULENCE MODELING IN KOLMOGOROV FLOW 595
INVESTIGATION OF LAMINAR STEADY AND UNSTEADY FLOWS IN GYROID TPMS STRUCTURES 603
DETAILED CHARACTERISATION OF PORE STRUCTURE AND TRANSPORT PROPERTIES OF BIOMASS PARTICLES DURING PYROLYSIS 609
INVESTIGATING THE INFLUENCE OF PARTICLE SHAPE ON THE PYROLYSIS OF THERMALLY THICK PARTICLES IN DEM /CFD 617
NUMERICAL AND EXPERIMENTAL INVESTIGATION OF LOW REYNOLDS NUMBER FLOW IN A PACKED BED OF ROTATED BARS 625
ENHANCING DEM-CFD SIMULATIONS WITH MACHINE-LEARNING-BASED LOCALLY RESOLVED NUSSELT NUMBER CORRELATIONS 633

AN OPEN WORKFLOW FOR UNSUPERVISED CLUSTERING OF FLUID-PARTICLE FLOWS INTO COMPARTMENTS 641
A COMPRESSIBLE TWO-FLUID MODEL FOR THE SIMULATION OF TRIBOELECTRIFICATION 648
INFLUENCE OF PACKING DENSITY ON THE CALCINATION PROCESS FOR LIME PRODUCTION: A DEM-CFD STUDY 656
MULTISCALE COMPUTATIONS OF REACTIVE MULTIPHASE FLOWS 664
OPTICAL THERMOMETRY COUPLED TO THE MEASUREMEN-T OF OTHER QUANTITIES (VELOCITY, PRESSURE) 677
MACROSCOPIC AND MICROSCOPIC BLOOD FLOWS 682
A LOOK BACK ON 30 YEARS OF TURBOMACHINERY RESEARCH IN EUROPE 690
Sponsors and Partners 716

*Conference on Modelling Fluid Flow (CMFF'25)*
*The 19th International Conference on Fluid Flow Technologies*
*Budapest, Hungary, August 26 - August 29, 2025*

# A 0D-3D MODEL FOR THE ANALYSIS OF THE TRANSIENT THERMAL BEHAVIORS OF AN ELECTRIC POWER TRAIN

Alessio SUMAN[1], Riccardo BONDESAN[2], Luca CONDOTTA[2], Lorenzo ANTONIOLI[2], Nicola ZANINI[2], Mattia BATTARRA[2], Emiliano MUCCHI[2], Mattia PIOVAN[2], Michele PINELLI[2]

[1] Corresponding Author. Department of Engineering, University of Ferrara, Ferrara, Italy. E-mail: alessio.suman@unife.it
[2] Department of Engineering, University of Ferrara, Ferrara, Italy. E-mail: first name.family name@unife.it

## ABSTRACT

Electric vehicles are recognized as the solution for the future to reduce emissions, especially in the city center, where health-related issues are due to the high population density and pollutant concentration. Due to this, the automotive industry has to change several paradigms to introduce more efficient vehicles and overcome the reluctance to change the user. In this sense, the thermal management of the vehicles has to be re-designed to manage the operating temperature of high-power devices such as drivers and motors. In the present investigation, a lumped parameter model has been developed to study the dynamic thermal behaviors of electric vehicle power trains. The study analyses the interaction between the heat exchanger and the operation of two electric motors and a single inverter. To set up the model, a computational fluid dynamics simulation has been carried out to characterize the thermal-fluid dynamic characteristics of the relevant components of the system, such as the cooling systems of the inverter and the electric motor. Stationary and transient analyses have been carried out considering the variation of the thermal load according to the vehicle route. The effects of thermal inertia and the effects of the control logic system have also been highlighted.

**Keywords: electric vehicle, thermal management, lumped-parameter model, computational fluid dynamics, dynamic simulations**

## NOMENCLATURE

| | | |
|---|---|---|
| $H$ | [bar] | pump head |
| $h$ | [W/m$^2$K] | heat transfer coefficient |
| $P$ | [W] | power |
| $p$ | [bar] | static pressure |
| $Q$ | [l/min] | volume flow rate |
| $T$ | [°C] | temperature |
| $t$ | [s] | time |
| $\Delta$ | [-] | difference |

## 1. INTRODUCTION

Thermal management of an electric vehicle is crucial to extend the rangeability and reduce electric consumption. Recent estimations show that the thermal management system accounts for 60 % of the total electric usage [1 – 3]. The modeling of such systems determines several challenges related to the cross-correlation between devices designed to accomplish different tasks (e.g., cabin temperature, heat rejection of the power train, etc.) [1]. To study such a system, low-order models help run several scenarios representing the operating conditions involved in automotive applications. Lumped-parameter models (LPM) are among the most known low-order models. The LPM model is based on a set of equations representing the physical phenomenon and, simultaneously, a set of coefficients or datasets representing the relationship between independent variables and the characteristics of each modeled device/system. Lumped parameter models allow the schematization of the system with details related to cross-correlation phenomena coming from the thermal systems, transmission, and driver characteristics [4, 5], showing the possibility of using the model to optimize the systems by reducing fuel consumption.

Similarly, LPM has been used to assess the interaction between electrical devices in electric-powered vehicles, showing the possibility of studying complex phenomena using low-order models [6]. The LPM could be fed by experimental data or numerical data obtained by high-order models such as computational fluid dynamic simulations. In [7], the LPM of a heat pipe based on CFD simulations is proposed. The three-dimensional simulations were used to estimate the heat transfer coefficients in a complex geometry. At the same time, the LPM results could be checked by CFD simulations, increasing the usefulness of the LPM model to reduce the computational effort in the case of several simulating runs [8 – 10].

### 1.1. Aim of the paper

In the present paper, an LPM has been developed to study the thermal behavior of the electric power train of a single-seater racing car. The present results refer to the analysis of the cooling circuits designed for the racing car involved in the Formula SAE competition [11]. The present modeling process consists of a framework created using a lumped parameter model in which a set of data and parameters have been obtained by CFD simulations. The CFD analysis was used to characterize the on-purpose design component devoted to managing the thermal behavior of electric motors and inverter. Using the LPM, stationary and dynamic simulations were carried out to describe the cooling systems and assess temperature variation during an endurance test. In this scenario, the control logic based on temperature data can increase car efficiency, reduce consumption, and manage electric power trains.

## 2. COOLING CIRCUIT

The designed cooling circuit consists of numerous components designed or selected for this specific application. The full-electric racing car includes four electric motors (four-wheel drive concept) and a single inverter that manages the electric power supplied by the battery pack to the electric motor according to the driver's needs and circuit layout. To control the operating temperature of motors and inverter, the cooling circuit is composed of the following elements:

- recirculation pump;
- heat exchanger with cooling fan;
- water jacket for cooling the electric motor;
- cold plate for cooling the inverter;
- rubber hose and fittings.

The cooling circuit and its devices have been reported in a three-dimensional layout proposed in Fig. 1. A recirculating pump supplies the flow rate through the cold plate. After that, the tee fitting was placed to split the water flow rate into two water jackets to cool down the electric motor. After the water jacket, the two lines were re-joined immediately before the heat exchanger. This layout was implemented in the LPM by using Simcenter Amesim software.

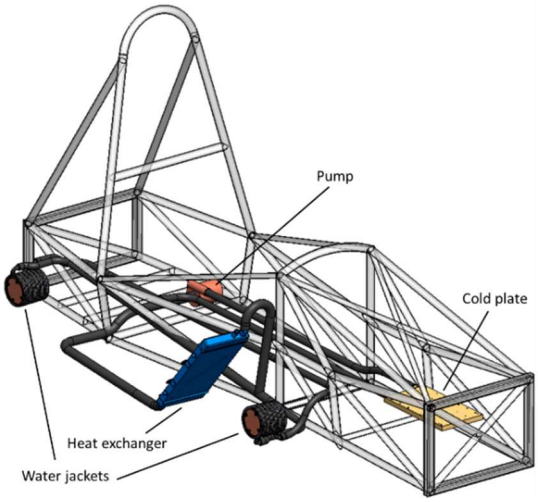


**Figure 1. The cooling circuit layout**

## 3. COMPONENTS CHARACTERIZATION

In the following paragraphs, the characterization of the relevant devices has been reported to create the most representative LPM of the cooling circuit.

### 3.1. Pump, heat exchanger and fittings

The pump and the heat exchanger were selected from the market based on their performance, space requirements, and weight. Such components were characterized by manufacturers, and in this section, only the relevant characteristics related to the LPM have been reported.

The pump performance (provided by Vovyo Technology Co., LTD.) is reported in Fig. 2 according to the flow rate versus head. Since the competition rules impose water as cooling media, the characteristics curve used in the LPM corresponds to that reported in Fig. 2.

Regarding the heat exchanger, the AKS DASIS model DASIS320100N has been selected for the present application. The heat exchanger has a heat rejection value of 10 kW. Such a value is greater than the estimated thermal power that has to be exchanged. However, installing the heat exchanger in the car's side pods determines the nominal air flow rate reduction, reducing the heat exchanger capability. The heat exchanger has been coupled with a circulating fan to ensure the greatest safety of the electric circuits. The fan is the type VA14-BP7 from the manufacturer SPAL Automotive Spa. In the present design, the fan activation is controlled by a control logic based on the temperature value measured in correspondence with critical devices such as the electric motor and inverter. Such a condition will be implemented in the LPM to study the most severe condition of the circuits.

Finally, the connection between the devices has been described. According to Fig. 1, the cooling circuit develops according to the car length, from the

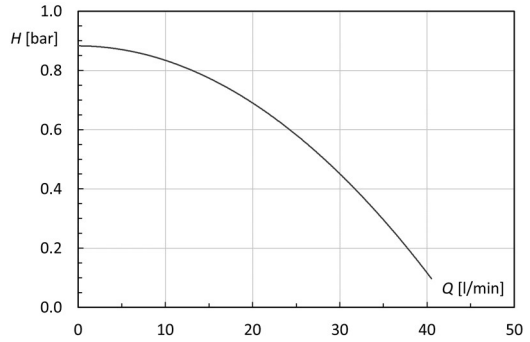


**Figure 2. Pump performance: head (*H*) versus flow rate (*Q*)**

rear to the front section. The circuit consists of pipes suitable for hot water delivery, mainly used as a flexible connection in the cooling circuits of automotive engines. They are made of black EPDM rubber with synthetic textile reinforcing inserts inside to overcome the pressure.

### 3.2. Water jacket

The water jacket is used to cool the electric motor. Using a water jacket is known in the literature as a good solution to manage the temperature of electric motors, increasing efficiency and reliability. In [12, 13], analyses of different water jackets designed for cooling the electric motor are reported. In the present analysis, the water jacket's specific design must be accounted for. The water jacket is designed to adhere externally to the electric motor. It is characterized by a coil that wraps around them through which the cooling fluid flows. The external surface of the electric motor is smooth, allowing a sealing process with grooves in the water jacket. Therefore, the cooling water is directly in contact with the electric motor and is supplied through the water jacket in a spiral shape. In Fig. 3, the three-dimensional shape of the designed water jacket and the sketch with relevant dimensions are reported. It is realized using a 3D printer process and PA 12 material filled with carbon fiber.

The water jacket performance was discovered through CFD simulations. A numerical analysis is mandatory to find the relationship between water flow rate and performance data, such as pressure losses and heat exchange parameters. To do this, a numerical model was setup. The computational domain comprises the electric motor external surface and the entire geometry of the water jacket reported in Fig.3. The model setup is similar to that described in [14]. The calculation is based on commercial Flow Simulation software embedded in the Solidworks suite. The computational model is discretized using a cut-cell approach by 530k Cartesian-grid elements while the low Reynolds number k–ε model, as in the Lam–Bremhorst formulation, is used [15]. A proper independent grid analysis was performed to assess the model's reliability. A refinement ratio 1.2 was used, and the selected mesh was the finest. A deviation from the coarsest grid (370k elements) and the finest (530k) was estimated to equal 6.3 % on the water jacket pressure drop. The spatial derivatives are approximated with implicit difference operators of second-order accuracy. The CPU time for the finest grid was 2 h on a workstation equipped with 8 physical processors.

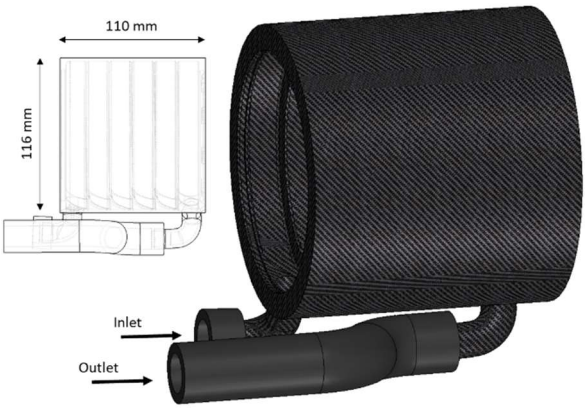


**Figure 3. Water jacket to cool the electric motor**

A volume flow rate value was imposed at the inlet section, while a static gauge pressure equal to 0 Pa was imposed at the outlet section. Three representative volume rates have been used to characterize the thermal behavior equal to 4, 8, and 12 l/min. From the CFD simulations, the heat transfer coefficient at the electric motor surface and the water jacket pressure losses have been assessed. In Fig. 4, the contour plot of the heat transfer coefficient obtained for the highest flow rate value is reported. Table 1 reports the CFD results helpful to represent the water jacket performance in the LPM as a function of the volume flow rate $Q$. Pressure losses ($\Delta p$) are intended as the difference between the static pressure at the inlet and the outlet. The heat transfer coefficient ($h$) is intended as the average value on the electric motor surface.

### 3.3. Cold plate

The inverter gets significantly overheated during the operation at the full power. The latter is placed on top of a cold plate to dissipate the heat developed by the inverter. This is an aluminum alloy plate traversed on the inside by tubes through which the cooling fluid passes. The design of the cold plate is reported in Fig. 5. It was provided by the manufacturer of the inverter (AMKmotion GmbH), who reported the proper fittings for the inverter and

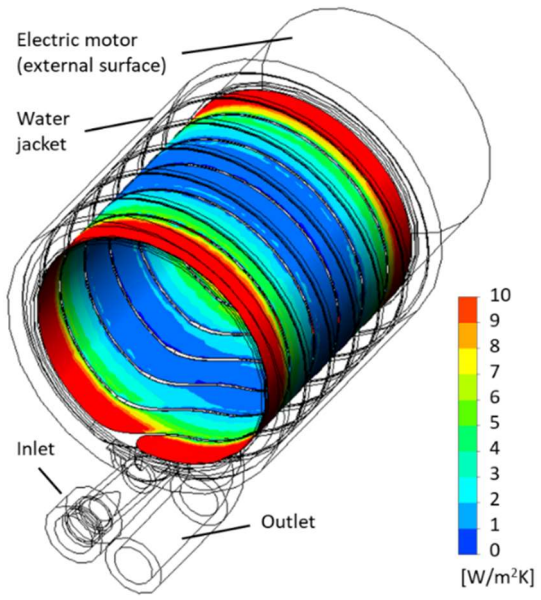


**Figure 4. Heat transfer coefficient at the electric motor surface (12 l/min)**

**Table 1. Water jacket performance**

| $Q$ [l/min] | $\Delta p$ [bar] | $h$ [W/m$^2$K] |
|---|---|---|
| 4 | 0.01 | 7.6 |
| 8 | 0.05 | 8.3 |
| 12 | 0.11 | 8.6 |

all the electrical devices. The cold plate is made of aluminum alloy (AlMgSi0.5), and an internal circular-shaped groove characterizes it.

Similar to the previous analysis, the cold plate has to be characterized in terms of pressure drop and heat exchange performance. A numerical model has been defined in line with the model proposed for the water jacket (software suite, turbulence model, and boundary conditions). A cut-cell approach by 400k Cartesian-grid cell has been used. A similar analysis related to the grid independence analysis was adopted. Even in this case, a refinement ratio of 1.2 was used, and the deviation between the coarsest and the finest (selected) grid was 3.2 % for the cold plate pressure drop. The CPU time for the finest grid was 1.5 h on a workstation equipped with 8 physical processors. The cold plate performance was computed for three different volume flow rate values equal to 8, 16, and 24 l/min. In Fig. 6, the contour plot of the heat transfer coefficient obtained for the highest flow rate value is reported. Table 2 reports the CFD results helpful in representing the cold plate performance in the LPM.

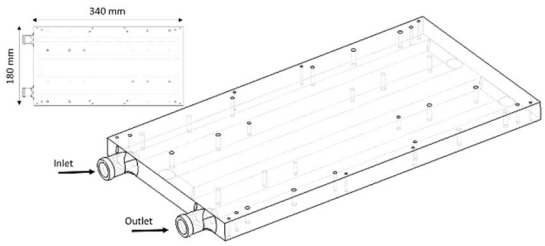


**Figure 5. Cold plate design**

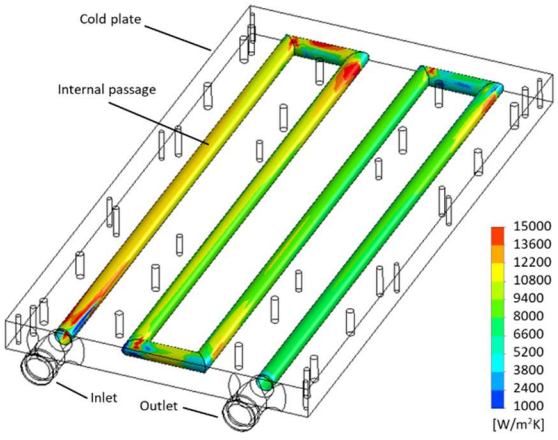


**Figure 6. Heat transfer coefficient at the cold plate internal passage (24 l/min)**

**Table 2. Cold plate performance**

| $Q$ [l/min] | $\Delta p$ [bar] | $h$ [W/m$^2$K] |
|---|---|---|
| 8 | 0.18 | 4046 |
| 16 | 0.46 | 6491 |
| 24 | 1.01 | 8879 |

## 4. LUMPED PARAMETER MODEL

After the component characterization, the LPM can be assembled. The LPM comprises libraries and specific blocks used to define the behavior of relevant components. The LPM has been created in the Simcenter Amesim environment. The first step is to select the proper libraries. In this project, five libraries have been used:

- *Cooling system*: this library includes a set of specific components fully compatible with the *Thermal Hydraulic* and *Thermal* libraries useful to study cooling systems in which temperature variation and fluids are involved;
- *Thermal Hydraulic*: this library is dedicated to designing hydraulic systems in which fluid temperature variations greatly influence the overall system behavior. It is based on a transient heat transfer approach used to model thermal phenomena in liquids (energy transport, convection) and to study the thermal evolution of these liquids in a hydraulic system;
- *Thermal*: this library deals with modeling heat transfer phenomena (conduction, free and forced convection, and radiation) involving solid materials;
- *Thermal Hydraulic Resistance*: this library is dedicated to the analysis of the evolution of pressure drops and flow rates in hydraulic networks where changes in fluid temperature have a significant influence on the overall behavior of the system being modeled;
- *Signal Control*: this library describes the power signal characterizing the inverter and electric motors.

After defining the proper libraries, a block was selected to create the adequate boundary condition and modeling strategy for the relevant components.

The boundary conditions blocks are listed as follows:

- THSD00: to define the materials of the devices (cold plate and water jackets);
- CSMP1: represents the mission profile. This block helps study both stationary (100 km/h, 600 s) and dynamic conditions (endurance test);
- CSES0: to define the ambient condition of the simulation;
- CSED0: to define the vehicle data;
- TFFD3: to define thermal-hydraulic

properties.

Specific blocks were used to model the relevant components. The description of such blocks is reported in the following paragraphs.

### 4.1. Pump, heat exchanger, and fittings models

The recirculating pump was modeled by the TFPUC0 block (*Thermal-hydraulic resistance* library) coupled with a PM000 electric motor to realize the assembly called the *electric pump*. The motor block allows the modification of the pump rotational speed if required. The pump performance curve (volume flow rate versus head) was added by using the AMETable subprogram. This curve is expressed through discrete values obtained from the manufacturer (see Fig. 2).

The most appropriate solution to model the heat exchanger is based on the CSRA022 block. Two additional blocks were used to increase the reliability of the present model. The TRIG0 block allows, being connected to a temperature sensor at the radiator's output, to detect if the temperature in the radiator is getting too high (above a threshold value imposed by the user) and consequently give the input to activate the fan. The CSDATA000 block helps in the specification of vehicle velocity (e.g., the air velocity on the radiator surface).

Using the layout proposed in Fig. 1, the tube length and diameter have been assessed. To model the cooling circuit in terms of length and fittings (bend, tee, etc.), the following blocks have been used:

- TFL000: used for straight pipe;
- TFBP11: used for bend;
- TFDC10: used for diameter changes;
- TF206: used for three-way fitting.

### 4.2. Water jacket and cold plate models

The water jacket and the cold plate have been modeled by the CSEN032 block. Such a submodel allows the definition of the heat flow source and a heat flow rate, which are specified according to the data related to inverter and electric motor heat generation. In stationary conditions, such a value will be kept constant. In contrast, in dynamic simulation, the values of the heat flow rate will vary according to the power consumption related to the endurance test. In addition to these data, the heat transfer coefficient is mandatory, representing the heat exchange process between the coolant fluids (simulated in the LPM) and the electrical devices (inverter and electric motor). These numbers were obtained by the CFD simulations, and they are reported in Tables 1 and 2.

## 5. STATIONARY CONDITION

A sensitivity analysis of the LPM was performed to evaluate the cooling circuit's performance in several operating conditions (thermal power, vehicle speed, cooling flow rate, etc.). In the present manuscript, a representative stationary condition has been reported. The ambient temperature has been set at 36 °C (summer condition), while the threshold temperature for the cooling fan is imposed equal to 65 °C. The thermal power at the cold plate was equal to 2000 W, while at the electric motor, a thermal power of 1200 W was imposed. The vehicle speed was imposed equal to 100 km/h, representing the condition in which the estimated maximum speed is reached using the maximum of the inverter and the electric motor. The results of the LPM model allow the identification of the operating point of the cooling pump and the related head that overcomes the pressure losses over

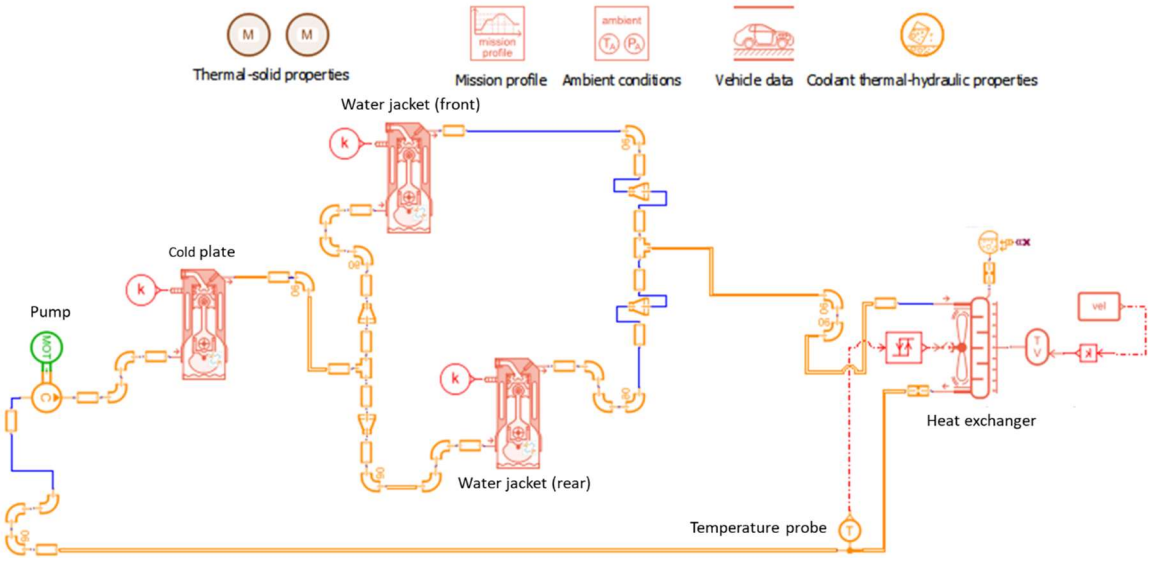


**Figure 7. LPM of the cooling circuit realized in the Simcenter Amesim environment**

**Table 3. Results of the stationary simulation**

| Component | $\Delta p$ [bar] | $\Delta T$ [°C] |
|---|---|---|
| Water jacket | 0.056 | 1.8 |
| Cold plate | 0.619 | 1.5 |
| Heat exchanger | 0.002 | 3.3 |
| Pump head | 0.721 | 0.0 |

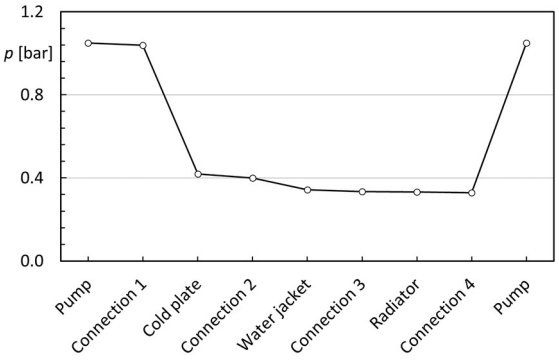


**Figure 8. Pressure trend over the cooling circuit**

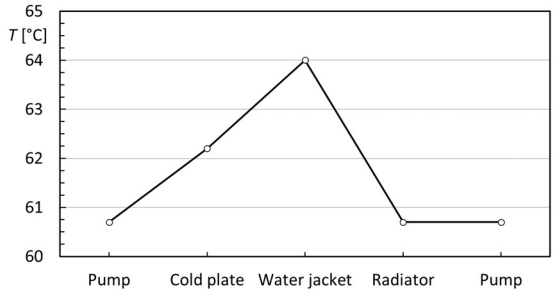


**Figure 9. Temperature trend over the cooling circuit**

the circuit. Similarly, the temperature difference across each component can be obtained. The results are reported in Table 3. Figures 8 and 9 report the pressure and the temperature values over the cooling circuits. The charts show the pressure and temperature values according to the cooling water flow path, which starts from the pump outlet section.

From the results obtained in the stationary condition for the worst scenario, it is possible to draw several indications. The internal pressure is lower than the critical value reported for each component and suitable for the selected rubber hose.

Similarly, the highest temperature is lower than the critical values for pure water. At the same time, the working temperature values of the electrical device (inverter and motor) are within the safe range defined by the manufacturer. At the same time, the temperature differences obtained with the LPM simulation are lower than the critical values ($\Delta T < 5$ °C for cold plate and water jacket).

## 6. DYNAMIC SIMULATION

A dynamic simulation was carried out using the LPM in order to simulate the car performance during the endurance test, with particular attention paid to the behavior of the cooling system during the execution of subsequent identical laps.

The first step is the definition of the typical lap. From the data previously recorded by the racing team, a typical is 1 km long and repeated 22 times. In addition to this overall data, the electrical power for the inverter and electric motor have been assessed. These data represent the thermal load of the cooling circuits, which change according to the lap layout (straights and curves). Using the mission profile block (CSMP1), the sequence of straights and curves (15 steps) regarding thermal power and vehicle velocity has been reproduced. In Fig. 10, the mission profile regarding vehicle speed has been reported. The maximum speed is reached at the end of the straight, while the average velocity is between 50 km/h and 60 km/h. The vehicle speed is divided into 15 steps and is the basis for estimating the thermal input for the cooling circuit.

The electrical power and vehicle speed can be matched by using the datasheet provided by the manufacturer. The calculation estimated the current intensity coupled to the voltage values for the electrical motor and, thus, the water jackets. The combination of these values results in the thermal power profile proposed in Fig. 11. It is important to note that the thermal power experienced at the inverter section follows the trend of the water jacket and vice versa. This is due to the correlation between

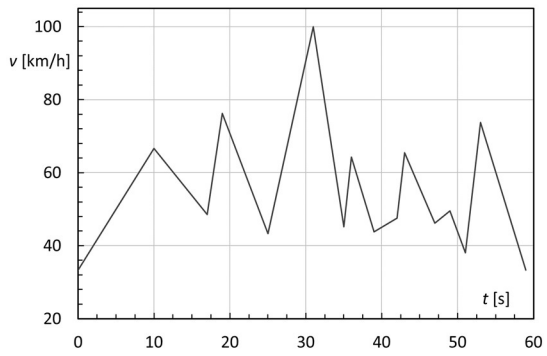


**Figure 10. Mission profile: vehicle speed**

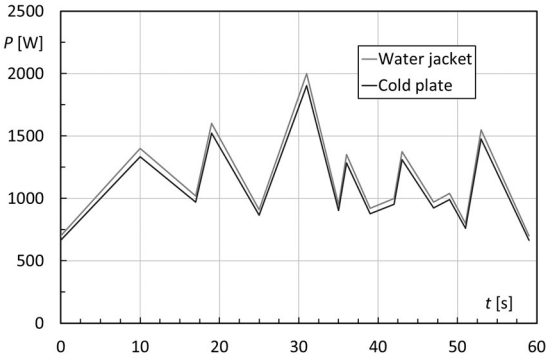


**Figure 11. Mission profile: thermal input at the cold plate and water jacket**

the power supplied by the inverter and the electric power at the motor. Such a condition determines that the cooling circuit has to overcome the contemporary presence of the highest values of thermal input in both the cold plate and water jacket.

The last required data for the dynamic simulation is the initial condition. Since no data are available, the initial condition will be kept equal to the worst scenario, as represented by the stationary condition that was reported early. This allows the cooling circuit performance to be evaluated when it operates at full load immediately before the start of the endurance test.

Figures 12 – 15 report the temperature trend obtained during the simulation of the endurance test. Figures 12 – 14 refer to the temperature values obtained in correspondence with the inlet and outlet sections for the water jacket, cold plate, and heat exchanger. It can be noted that after the initial phase (which is estimated to be 8 laps long), the cooling circuit achieves a cyclic condition characterized by the repetitive sequence of straight and curves described with the mission profile reported in Fig. 10. All temperature differences remain approximately constant, and the proper performance of the system is constantly verified and satisfied, ensuring adequate heat removal from the inverter and electric motors during the endurance test.

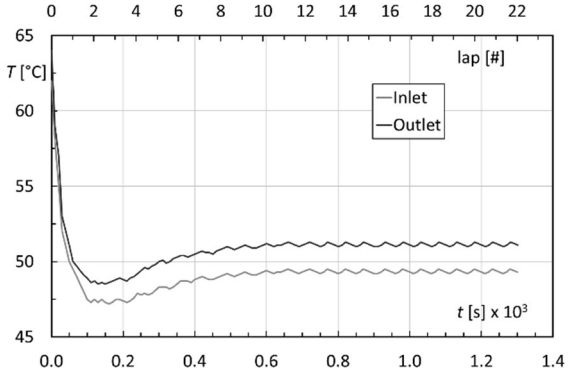


**Figure 12. Inlet and outlet temperature trends for the water jacket during the endurance test**

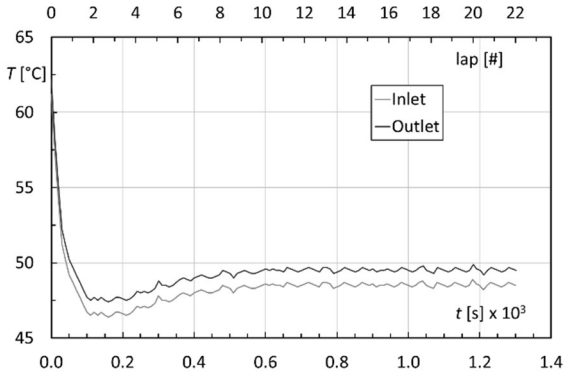


**Figure 13. Inlet and outlet temperature trends for the cold plate during the endurance test**

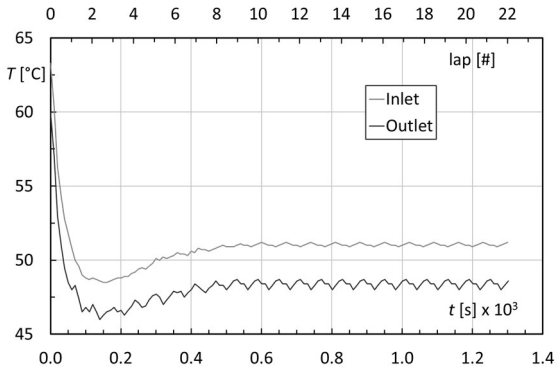


**Figure 14. Inlet and outlet temperature trends for the heat exchanger during the endurance test**

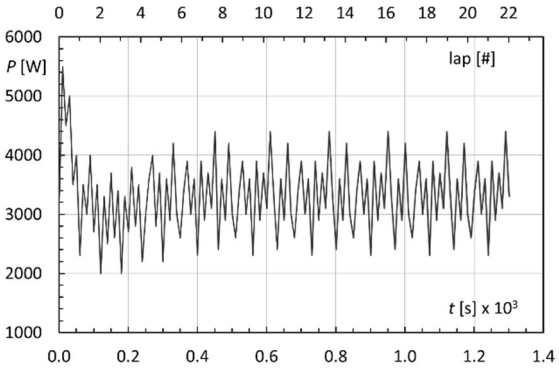


**Figure 15. Thermal power trends at the heat exchanger during the endurance test**

Figure 15 shows the thermal power exchanged by the radiator. The local variations (peaks and valleys) are visible due to the instantaneous variation of the thermal inputs. At the same time, an almost constant average value of the thermal power can be seen, approximately 3500 W.

## 7. CONCLUSIONS

In the present analysis, a lumped parameter model has been used to assess the stationary and dynamic performance of a cooling circuit used in an electric car. The present design refers to the thermal management of an electric powertrain used in a single-seater racing car.

The modeling process involves the schematic representation of the three-dimensional layout of the circuits and the analysis of the devices devoted to cooling the inverter and the electric motors. In particular, the designed-on-purpose cold plate (for the inverter) and the water jacket (for the electric motor) were characterized using CFD simulations. The LPM model has been completed by adding the manufacturer's pump and heat exchanger data.

After defining the library set and the most suitable block, a stationary simulation was performed. The worst scenario regarding operating temperature and thermal power input has shown that the cooling circuit allows the preservation of the

operating characteristics of devices, matching the safe condition provided by the manufacturer. Starting from the stationary condition, a dynamic simulation was set up to study the cooling circuit performance during an endurance test. The model results show the temperature and the thermal power trends according to the laps. Even starting from the conditions related to the maximum thermal load, the cooling circuit can overcome the endurance test, ensuring suitable thermal management of the entire system.

Using the methodology presented in the present work, it is possible to check the system's reliability during the design phase and, simultaneously, increase the efficiency of the vehicle, reducing the consumption and thus increasing the rangeability or the performance of the entire vehicle.

## ACKNOWLEDGEMENTS

This work has been carried out in the framework of the regional grant N. 2/2023 “Invito agli atenei e agli istituti afam a presentare progetti “team di sviluppo di prototipi/soluzioni per la partecipazione a competizioni nazionali e internazionali”, founded by Emilia Romagna region. The authois wish to thanks Siemens Industry Software srl, and Frig Air Spa for their support.

## REFERENCES

[1] Zhao L., Zhou Q., Wang Z. A systematic review on modelling the thermal environment of vehicle cabins (2024) *Applied Thermal Engineering*, Vol. 257, art. no. 124142

[2] Wang X., Li B., Gerada D., Huang K., Stone I., Worrall S., Yan Y. A critical review on thermal management technologies for motors in electric cars (2022) *Applied Thermal Engineering*, Vol. 201, art. no. 117758

[3] Carriero A., Locatelli M., Ramakrishnan K., Mastinu G., Gobbi M. A Review of the State of the Art of Electric Traction Motors Cooling Techniques (2018) *SAE Technical Papers*, 2018-April

[4] Ganesan A., Jaiswal R., Pitchaikani A. A Study of an Integrated HVAC-Vehicle Model for Automotive Vehicles (2018) SAE *International Journal of Passenger Cars - Mechanical Systems*, Vol. 11 (2), pp. 151 – 166

[5] Huang Y., Khajepour A., Bagheri F., Bahrami M. Modelling and optimal energy-saving control of automotive air-conditioning and refrigeration systems (2017) *Proceedings of the Institution of Mechanical Engineers, Part D: Journal of Automobile Engineering*, Vol. 231 (3), pp. 291 – 309

[6] Chen B., Wulff C., Etzold K., Manns P., Birmes G., Andert J., Pischinger S. A Comprehensive Thermal Model for System-Level Electric Drivetrain Simulation with Respect to Heat Exchange between Components (2020) InterSociety Conference on Thermal and Thermomechanical Phenomena in Electronic Systems, ITHERM, 2020-July, art. no. 9190448

[7] Bernagozzi M., Charmer S., Georgoulas A., Malavasi I., Michè N., Marengo M. Lumped parameter network simulation of a Loop Heat Pipe for energy management systems in full electric vehicles (2018) *Applied Thermal Engineering*, Vol. 141, pp. 617 – 629

[8] Akawung A.F., Fujimoto Y. Thermal Analysis of Air Cooling System for Electric Machines Using Lumped Parameter and Flow Resistance Network (2021) IEEE International Symposium on Industrial Electronics, 2021-June

[9] Grunditz E.A., Lundmark S.T., Alatalo M. Evaluation of three cooling concepts for an electric vehicle motor - Lumped parameter models (2020) Proceedings - 2020 International Conference on Electrical Machines, ICEM 2020, art. no. 9271015, pp. 860 – 866

[10] Stuppioni U., Natali C., Battarra M., Blum A., Suman A., Pinelli M., Dalpiaz G., Mucchi E. Experimental and numerical characterization of the under-vane pressure in balanced vane pumps (2024) *Results in Engineering*, Vol. 23, art. no. 102439

[11] Formula ata (2024) https://www.formula-ata.it/formula-sae-italy/, accessed 30th december, 2024

[12] Satrústegui M., Martinez-Iturralde M., Ramos J.C., Gonzalez P., Astarbe G., Elosegui I. Design criteria for water cooled systems of induction machines (2017) *Applied Thermal Engineering*, Vol. 114, pp. 1018 – 1028

[13] Grunditz E.A., Lundmark S.T., Alatalo M. Evaluation of three cooling concepts for an electric vehicle motor - Lumped parameter models (2020) Proceedings - 2020 International Conference on Electrical Machines, ICEM 2020, art. no. 9271015, pp. 860 - 866

[14] Pinelli M., Suman A. Thermal and fluid dynamic analysis of an air-forced convection rotary bread-baking oven by means of an experimental and numerical approach (2017) *Applied Thermal Engineering*, Vol. 117, pp. 330 – 342

[15] Lam C.K.G., Bremhorst K. A modified form of the k-ε model for predicting wall turbulence (1981) *ASME J of Fluids Engineering*, Vol. 103 (3), pp. 456 - 460